

Low-Pass Cascade Filters with High Attenuation Rate in the Stopband

Vratislav MICHAL¹, Jiří SEDLÁČEK², Karel HÁJEK³

¹ LGEP-Supélec, Université Pierre et Marie Curie - Paris 6; 11 rue Joliot-Curie, Gif-sur-Yvette, France

² BUT, Department of Theoretical and Experimental Electrical Engineering; Kolejní 2906/4, Brno, Czech Republic

³ University of Defence, Department of Electrical Engineering; Kounicova 65, 612 00 Brno, Czech Republic

vratislav.michal@supelec.fr, sedlacj@feec.vutbr.cz, karel.hajek@unob.cz

Abstract. In this paper, we present two biquadratic structures for cascade filter design, which are intended to provide high attenuation rate in the stopband area of frequency transfer characteristic. The filters optimized in this way can reach better electrical performances, such as higher maximal cut-off frequency or dynamic range, even with conventional (low power consumption) active devices. We present a modification of the well-known Sallen-Key filter and a biquadratic filter based on the second generation current conveyor CCII-. Presented approach relies on the elimination of parasitic transfer zeros in the real transfer function, which are caused by the non-ideal parameters of real active elements. Their impact is eliminated by unconventional definition of the filter output.

Keywords

Active low-pass filter, Sallen-Key, CCII, attenuation floor, biquadratic filter, real operational amplifier.

1. Introduction

The using of the low-pass frequency filters is intended to suppress signals located above the cut-off frequency f_0 , while the signals located in the pass-band are to be transmitted. However, the suppression rate is limited for many real active filters, namely at higher frequencies. This is mainly due to the non-ideal parameters of real active elements, for instance to a limited bandwidth and nonzero output impedance of an operational amplifier. In this case, we observe parasitic zeros in the transfer function, causing degradation of the ideal -40 dB roll-off slope and consequent spurious transfers [1]. A possible solution is to employ a component with better high frequency performances, this however leading to increased power consumption. On this account, the using of the structures with optimized high frequency parameters is recommended. For instance, we can prefer to use the OTA-C or MFB filters [2], since they contain grounded capacitors. However, the use of these filters can be inconvenient, e.g. due to the temperature dependency or

nonlinearity of OTA or undesirable phase shift 180° of the MFB biquad. Generally, the structures with good high-frequency behavior are built of higher number of active elements and their realization is therefore less economical.

In order to design optimized filter structures, we focus on the factors responsible for the increased transfer in the stopband. Consequently, we present two circuits: modified Sallen-Key filter in section 2 and CCII based biquad in section 3. Their high frequency parameters are optimized via the elimination of parasitic zeros in the real transfer function, provided by removal of the active component from the signal path at high frequencies. The required attenuation is ensured by a passive RC circuit.

2. Type II Sallen-Key filter

A commonly used block in the cascade filter design is the Sallen-Key (S-K) circuit, originally presented in [3] and shown in Fig. 1.

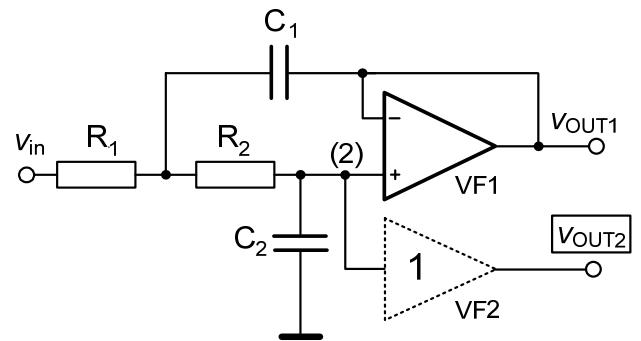


Fig. 1. Sallen-Key low-pass filter with low impedance output (V_{OUT1}) [2] and with buffered node (2) V_{OUT2} (type II S-K).

The cut-off frequency f_0 and quality Q factors are given in the well-know form:

$$f_0 = \frac{1}{2\pi\sqrt{R_1 R_2 C_1 C_2}}; \quad Q = \frac{\sqrt{C_1}}{\sqrt{C_2}} \frac{\sqrt{R_1 R_2}}{R_1 + R_2} = \frac{1}{2} \sqrt{\frac{C_1}{C_2}} \Big|_{R_1=R_2} \quad (1)$$

In order to achieve the low relative sensitivities ($S_{\Omega, Q} < 1$) and unity gain in the pass-band, the filter is usually

designed with an operational amplifier in the unity gain configuration (Fig. 1).

2.1 High frequency behavior of S-K filter

The properties of real Sallen-Key filter can, however, differ significantly from what was originally intended by the design. This is mainly due to the mentioned non-ideal parameters of real active elements. These non-ideal parameters induce well-known circuit imperfections such as the cut-off frequency and quality factor shifts, together with previously mentioned parasitic zeros degrading the stopband attenuation. The shifts of f_0 and Q are analyzed *e.g.* in [1, 2] and can be compensated by a predistortion technique [4]. When focusing on the stopband area, an analysis can point out the signal path between the filter input and output, which increases the influence of the real operational amplifier. As indicated in Fig. 2, the input terminals of S-K filter is interconnected with the output node v_{OUT} through the passive elements R_1 and C_1 .

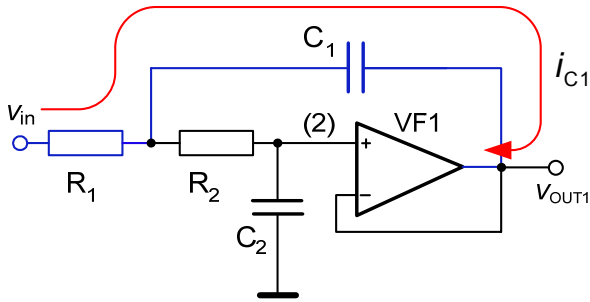


Fig. 2. The direct current path i_{C1} causing the parasitic zeros in the transfer function of real Sallen-Key filter.

The output of real voltage follower VF1 (v_{OUT}) exhibits an output impedance Z_{OUT} which increases when approaching the frequency limits of the operational amplifier. Therefore, the parasitic effects caused by the mentioned input-output interconnection are more pronounced at higher frequencies (the output of OA is intended to absorb the current i_{C1} ideally up to $f \rightarrow \infty$).

The influence of the real operational amplifier can be demonstrated by the analysis dealing with the 1st order OA model (we neglect the higher order effects as its modeling is highly inaccurate). We can deduce the presence of a parasitic triple zero of frequency f_{Z1} , where the attenuation attains its maximum level:

$$f_{Z1} \cong \frac{1}{2\pi} \sqrt[3]{\frac{A_0 \cdot \omega_p}{C_1 C_2 R_2 R_{OUT}}} \quad (2)$$

In this equation, A_0 is the DC gain, ω_p the dominant pole, and R_{OUT} the output resistance of the OA model. Above the frequency f_{Z1} , the transfer magnitude starts to increase with a positive trend of 20 dB/decade.

2.2 Increasing of the stopband attenuation

In order to achieve required high attenuation rate of the S-K filter, the frequency f_{Z1} needs to be increased. Eq. (2) incites the use of an operational amplifier with better HF performance, however usually having higher power consumption. In [5], an additional pole realized by a passive RC network was added to the S-K filter, which results in constant 0dB/dec slope above the f_Z . In this case, one can prefer to base the design on the 3rd order cascade sections directly, as shown in [6].

A considerable increase of the stopband attenuation can be achieved by interruption of the direct signal path between the filter terminals v_{IN} and v_{OUT} (Fig. 2). As the voltage follower VF1 ideally exhibits unity gain, the output voltage is also present on its input voltage node labeled (2). In this node, the current i_{C1} (Fig. 2) is interrupted by zero reverse transfer of VF1, and the high suppression is ensured by a passive circuit $R_2 C_2$. We can thus expect a higher attenuation achieved in the node (2) than at the output of classical S-K filter v_{OUT1} (Fig. 1).

The high frequency transfer $v_{(2)}/v_{IN}$ can be expressed similarly as in Eq. 2 (by means of the 1st order OA model), which results in a double parasitic zero of frequency f_{Z2} :

$$f_{Z2} \cong \frac{1}{2\pi} \sqrt{\frac{A_0 \cdot \omega_p}{C_1 R_{OUT}}} \quad (3)$$

The frequency f_{Z2} is therefore determined by the OA model parameters and the only passive element: capacitor C_1 . A rough trade-off between f_{Z1} (Eq. 2) and f_{Z2} (Eq. 3) favors f_{Z2} because of the low output resistance R_{OUT} and reduced root order. Therefore, classical Sallen-Key filter can be considerably improved by connecting an additional voltage buffer into the node (2), as shown in Fig. 1.

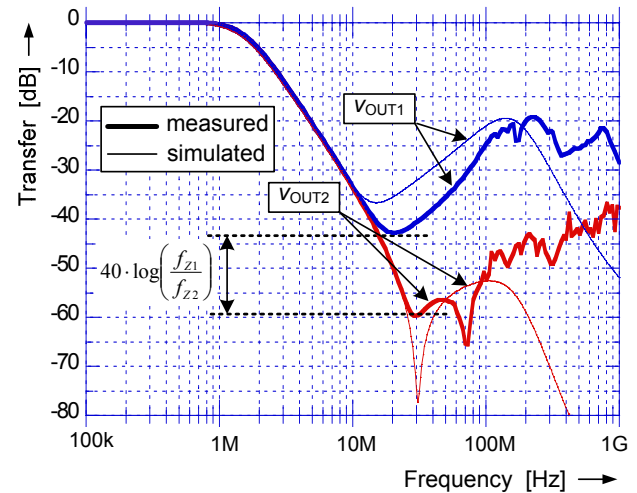


Fig. 3. Measured and simulated frequency characteristic of Sallen-Key filter with standard output v_{OUT1} and type II Sallen-Key (v_{OUT2}) filter with increased suppression (measured for $R_1 = 168 \Omega$, $R_2 = 100 \Omega$, $C_1 = 1.2 \text{ nF}$, $C_2 = 560 \text{ pF}$, OA = AD8055).

Indeed, the characteristics shown in Fig. 3 obtained by the measurement and simulation of filter designed for $f_0 = 1.5$ MHz and $Q = 1/\sqrt{2}$ exhibits higher attenuation rate for the type II S-K filter. Moreover, Eq. 3 shows a methodology allowing further increasing of the attenuation, simply by locating the parasitic zero f_{z2} to higher frequency (thanks to C_1 determining the filter impedance level).

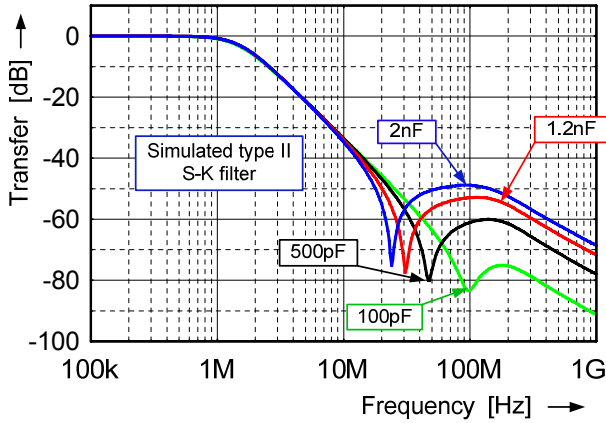


Fig. 4. Simulations of Sallen-Key type II filter designed for various impedance levels (Tab. 1). Simulations were performed with the AD 8055 SPICE model.

The effect of different filter impedance levels is shown in Fig. 4, where a positive impact of the low C_1 value can be observed (however, its excessive decrease can provoke secondary parasitic effects). The curves are marked by values of C_1 referring to the components ordered in Tab. 1.

C_1 (nF)	C_2 (nF)	$R_1 = R_2$ (Ω)	f_{z2} (MHz)
2.0	1.0	75	24.1
1.2	0.60	125	31.0
0.50	0.25	300	47.5
0.10	0.05	1.5k	95.1

Tab.1: The components' values of simulation shown in Fig. 4.

3. CCII- Biquadratic Section without Parasitic Zero

A biquadratic filter containing no parasitic zero in the real transfer function ideally reach constant roll-off slope of -40dB/dec, reduced only by the parasitic leakage of the input signal. The constant attenuation slope of -40dB/dec can be realized by a 2nd order RC filter. However, the RC filters reach only a low value of quality factor ($Q < 0,5$). A solution improving the high frequency performances would be therefore to divide the frequency bandwidth between the active component and passive circuit; the active component provides the resonance gain Q and transfer up to f_0 , whereas the passive circuit allows reaching required attenuation up to very high frequencies.

The presented network makes use of the second generation current conveyor (CCII-) containing three terminals: low impedance voltage output X , high

impedance voltage input Y , and current output Z ; the transfers between terminals are defined as: $v_X = v_Y$, $i_Z = -i_X$ and $i_Y = 0$ [7]. The design of biquadratic section based on techniques presented in [8] is shown in Fig. 5. Here, the input voltage is connected to the low input impedance terminal X through the resistor R_1 and coupled with the current output Z according to $i_Z = -i_X$. The current source is loaded by the π -network composed of the resistor R_2 and shunt capacitors C_1 and C_2 .

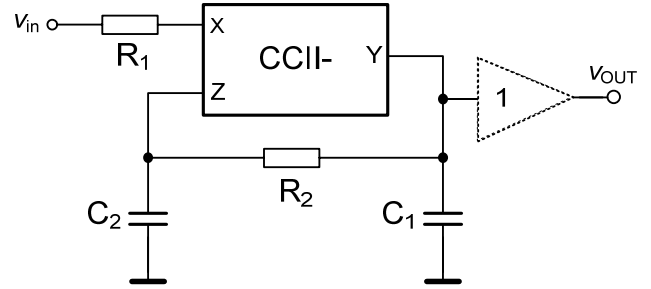


Fig. 5. The low-pass CCII- biquadratic filter reaching high attenuation in the stopband.

The filter is characterized by the cut-off frequency f_0 in typical form (Eq. 1) and the quality factor of:

$$Q = \frac{\sqrt{R_2}}{\sqrt{R_1}} \cdot \frac{\sqrt{C_1 C_2}}{C_1 + C_2} = \frac{1}{2} \sqrt{\frac{R_2}{R_1}} \Big|_{C1=C2} \quad (4)$$

In contrast to the Sallen-Key filter, the circuit from Fig. 5 has ideally no direct signal path from the input node v_{IN} to the output v_{OUT} . A potential direct signal path is interrupted by zero reverse transfer of the voltage follower between the CCII terminals X and Y . The stopband attenuation -40dB/dec is ensured by the passive π -network containing shunt capacitors. For this reason, terminal Y (located at the output of RC network) forms the filter output.

The high frequency performances of the filter can be demonstrated by the analysis dealing, for convenience, with a simplified model of the CCII. This model incorporates only a principal imperfection of CCII: real voltage follower. The voltage follower is modeled by the 1st order model of the operational amplifier (characterized by A_0 , ω_p and R_{OUT} , see sub-section 2.1), connected as unity gain amplifier. The frequency transfer v_{OUT}/v_{IN} of the filter results in the following (simplified) transfer function:

$$N(s) \cong \frac{\Omega_0^2}{(s^2 + s \cdot \Omega_0 / Q_0 + \Omega_0^2)} \cdot \frac{(\omega_p \cdot A_0 + s)}{(\omega_p \cdot (1 + \alpha) \cdot A_0 + s)} \quad (5)$$

where $s^2 + s \cdot \Omega_0 / Q_0 + \Omega_0^2$ is the standard 2nd order polynomial, and the parameter α is defined as $\alpha = R_{OUT}/R_2 \ll 1$. In Eq. 5, we can notice one nominator zero being eliminated by the denominator pole. Therefore, theoretical -40dB/dec roll-off slope in the stopband is achieved, and the attenuation floor is limited practically only by the mentioned parasitic signal leakage. A deeper

analysis was performed by means of simulation with the complex model of CCII. From this analysis, we can notice the importance of overlap capacity C_{X-Y} , which value needs to be minimized during the design.

The circuit's performances were also demonstrated by measurements of the 4th order Butterworth low-pass filter designed for cut-off frequency $f_0 = 10$ MHz. The frequency response shown in Fig. 6 reaches very good suppression going up to 100 dB. The current conveyor was realized by means of the CCII-K circuit [9].

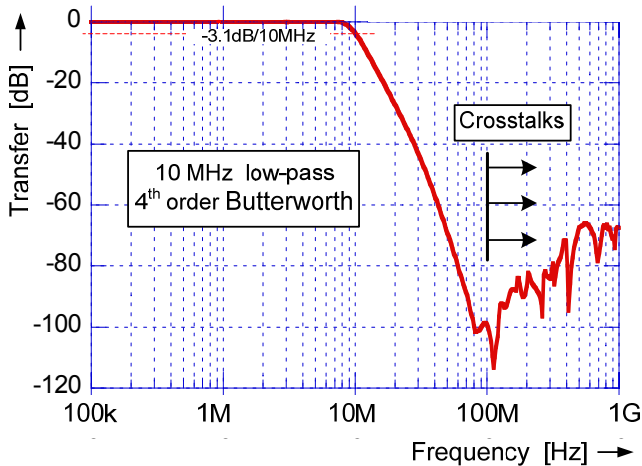


Fig. 6. Example of measured frequency response of the 4th order low-pass Butterworth filter realized by means of the CCII-K circuit [9] (OPA860 + AD8055).

The experimental measurements performed on a single 2nd order block (Fig. 5) confirm that the high suppression (above 60 dB) is independent of the designed cut-off frequency. Naturally, the good attenuation can only be achieved by a proper layout of the PCB respecting the general rules of RF design. In order to facilitate utilization of the filter, an integrated high performance CCII- current conveyor was developed in 0.35 μ m CMOS process and successfully tested.

4. Properties of voltage buffers

Although the supplementary voltage buffer is required in both presented filters (Fig. 1 and Fig. 5), factors concerning the basic electrical properties still belong to the class of Single Amplifier Biquads (SAB) [2]. The role of the additional voltage buffer is only to form a new low-impedance output, primarily in the pass-band area (*i.e.* only up to cut-off frequency f_0). On this account, the voltage buffer can use an OA with relatively low f_T frequency, which is advantageous for power consumption saving. In addition, the voltage buffer can be omitted when the filter is followed by any high input impedance stage (*e.g.* input of an A/D converter). Concerning the *type II* S-K filter, a proper choice of the voltage buffer VF2 can also contribute to the low DC offset voltage of the filter.

5. Conclusion

In this article, we analyze the main factors leading to the limited attenuation rate of conventional Sallen-Key low-pass frequency filter. This limitation is caused by the parasitic transfer zeros originating from the real parameters of the active elements. It has been shown that their impact depends significantly on the filter structure. As solution, we presented two optimized structures of active low-pass filters: modified type-II Sallen-Key and CCII- based filter. In these circuits, the parasitic transfers zeros are eliminated by the reduction of active element operations primarily only up to the cut-off frequency, whereas the required high and wideband attenuation is achieved by the passive RC network. The experimental results show that presented filters allow to reach improved electrical parameters; especially high maximal cut-off frequency or dynamic range. These improvements can be realized by using the active elements with low HF performances, which enable to reduce the power consumption as well as the final cost.

Acknowledgements

This research project has been supported by a Marie Curie Early Stage Research Training Fellowship of the European Community's Sixth Framework Program under contract number MEST-CT-2005-020692.

References

- [1] SCHMID, H., MOSCHYTZ, G.S. Fundamental frequency limitations in current-mode Sallen-Key filters. *Circuits and Systems*, 1998. June 1998, p. 57-60 vol.1.
- [2] HUELSMAN, L.P. Active and Passive Analog Filter Design: an Introduction. *McGraw-Hill Education*, ISBN: 0070308616, book Published: March 1993
- [3] SALLEN, R.P., KEY, E.I. A Practical method of Designing RC-Active Filters. *IEEE Trans. Circuit Theory*. Vol. 7, March 1955, p. 74-85.
- [4] GEFFE, P. R. Exact synthesis with real amplifiers. *IEEE Trans*. Vol. CAS-23, January 1976, pp.45-55
- [5] "Analysis of Sallen-Key Architecture", *Application note* Texas instrument SLOA024B, www.ti.com, July 1999
- [6] DUTTA ROY, S.C., MALIK, K.K. Active RC realisation of a 3rd order low pass Butterworth characteristics. *Electronics Letters*, Vol. 8, Issue 26, December 28 1972 Pages: 630 - 631
- [7] TOMAZOU, C., LIDGEY, F. J., HAIGH, D. G. Analogue Ic Design: The Current-Mode Approach., *EII Circuits and Systems Series*, Book 1993, ISBN-10: 0863412971
- [8] LIU, S.I., TSAO, H.T., WU, J., TSAY, J.H. Realizations of the single CCII biquads with high input impedance. *IEEE International Symposium on Circuits and Systems*, 1991, vol.3, June 1991
- [9] WAN L., NATARAJAN, S. Optimal design of CCII-K circuits for high frequency applications. *System Theory*, Mar 1995, p. 175 - 179
- [10] MARTINEK, P. Lossy FDNR based on CCII- current conveyor. *Proceedings on international conference Radioelektronika*, Brno, 2006